Research Article

Przemyslaw Lopato, Michal Herbko*, Ulrich Mescheder and Andras Kovacs

Influence of a thin dielectric layer on resonance frequencies of square SRR metasurface operating in THz band

https://doi.org/10.1515/eng-2022-0400
received October 19, 2022; accepted December 21, 2022

Abstract: This article investigates the effect of an additional thin dielectric layer on the top of the metasurface (MS), on the transmission of electromagnetic waves in the terahertz band. For this purpose, the split ring resonator-based MS was designed and analyzed in the terahertz band. The influence of permittivity, film thickness, and suspension height on S_{21} transmission coefficient characteristics was studied. For this purpose, a numerical model was created and solved using the finite element method. The conducted study can be helpful in three cases. First, changing the suspension height of the dielectric layer may allow tunable MSs using MEMS structures. Also, this research can be used to determine the effect of applying an additional layer of protection when using the MS as a sensor to test substances that can damage it. In addition, there is an opportunity to study the dielectric properties of thin films using the proposed MS.

Keywords: metamaterial, metasurface, split ring resonator, terahertz device, dielectric constant, material properties, coating, numerical analysis

*** Corresponding author: Michal Herbko,** Center for Electromagnetic Fields Engineering and High Frequency Techniques, Faculty of Electrical Engineering, West Pomeranian University of Technology, Szczecin, Poland, e-mail: michal.herbko@zut.edu.pl
Przemyslaw Lopato: Center for Electromagnetic Fields Engineering and High Frequency Techniques, Faculty of Electrical Engineering, West Pomeranian University of Technology, Szczecin, Poland
Ulrich Mescheder, Andras Kovacs: Institute of Microsystems Technology (iMST), Furtwangen University, Furtwangen im Schwarzwald, Germany

1 Introduction

Metamaterials are a new class of artificial compound materials, which exhibit exceptional properties not found in naturally occurring materials [1]. Specifically, it can be referred to ε-negative (ENG) or μ-negative (MNG) materials of either negative permittivity or permeability, respectively, double-negative (DNG) when both of these quantities are simultaneously negative in a specific frequency band, and ε-near-zero (ENZ) or μ-near-zero (MNZ) materials when these quantities have small, close to zero, values (this may be the case when the materials are near their electric or magnetic plasma frequency) [2]. These properties can be obtained by applying periodic or quasi-periodic arrays of sub-wavelength unit (structural) elements [3]. Much of the effort in the electrical engineering, material science, physics, and optics communities emphasized constructing efficient metamaterials and using them for potentially novel applications in antenna, sensor, and radar design, subwavelength imaging, and invisibility cloak design [4]. Currently, research is being conducted on the use of metamaterials and their planar version – metasurfaces (MSs) for different frequencies (from microwaves to visible light). An especially strong increase in interest is observed for the terahertz band. Terahertz MS application in communication technologies (6 G), sensors, and spectroscopy is anticipated and implemented [5–13]. Telecommunications systems operating at higher operating frequencies ensure faster data transfer, and for this reason, research is being conducted on new communication systems operating at terahertz frequencies [5,6]. To this end, there is a need to develop new solutions for antennas, filters, and terahertz lenses. The terahertz band is particularly important in studying chemical and biological substances with the use of the designed sensors. Examples of applications in which terahertz sensors were used are as follows: analysis of blood glucose [7], examination of cells for cancer [8], and the study of liquid crystal [9]. Terahertz spectroscopy has been developing in recent years. It has been used to test gases,

liquids, and solids, but researchers focus primarily on the study of liquids and solids. In the case of testing liquids, the sample should be placed in a measuring cell with a thickness of about 100 μm, due to the high water absorption capacity of terahertz waves. However, in the case of solids, terahertz spectroscopy is particularly useful in security control when detecting explosives and drugs [10]. Terahertz spectroscopy is used to study multilayer composite materials [11] or investigation of art [12]. In addition, spectroscopy is used to study emerging materials such as metal halides, perovskites, metal oxides, metal–organic frameworks, and 2D materials, due to the possibility of charge transport study [13].

One of the possible applications is an evaluation of thin layers. Earlier, thin films were measured using techniques like stylus profilometry, interferometry, ellipsometry, spectrophotometric measurements, and X-ray microanalysis [14–16]. Bolivar et al. [17] proposed using THz-TDS spectroscopy to determine the dielectric properties of materials. On the other hand, previous studies [18–20] proposed an eSRR MS for testing thin films. Park et al. [18] studied the influence of dielectric constant for the proper design of a microfluidic channel for liquid analysis. Analysis of liquids in the vicinity of the gap is possible due to the extremely confined electric field near the gap region of the MS. According to Park and Ahn [19], the use of a quartz substrate provides better distinguishability due to its lower refractive index [19]. Another example of studying dielectric properties is the use of a tunable MS using a MEMS-based comb driver. It can be applied in particular to the analysis of unconcentrated or live test materials [20].

In this work, an analysis of the influence of an additional thin dielectric layer in the vicinity of the MS on its properties was carried out, with particular emphasis on resonance frequencies. Such an analysis may concern three cases:

- the dielectric layer and changing its parameters act as a tuning mechanism influencing the configuration of MS (reconfigurable MSs);
- analysis of the influence of an additional dielectric layer (intended to protect the MS against the influence of external factors, e.g., when MS is part of a sensor of chemical or biological substances) on the properties of the MS;
- the additional dielectric layer acts as a thin tape, the properties/homogeneity of which we want to test (application in non-destructive testing, MS is a sensor illuminated with a terahertz beam).

This study aimed to investigate the effect of dielectric thin film on split ring resonator (SRR)-based MS. The transmission coefficient S_{21} (scattering matrix parameter) characteristics in the terahertz band for different thicknesses, suspension heights, and electrical permittivity of the dielectric layer were studied. The analysis of these three variables allowed for a more comprehensive look at the impact of the additional layer, which made it possible to propose potential applications and their limitations, something that has not been presented in the literature so far. For this purpose, an SRR-based structural element was designed, and a numerical model was built in the Comsol Multiphysics environment and solved using the finite element method (FEM). The results obtained will allow a better understanding of the impact of an additional thin layer, the use of the sensor, and to study the properties of thin films.

2 MS design

To design the SRR MS, a top-down assumption was made: the first resonance frequency f_{r1} = 1 THz, and the second f_{r2} < 3 THz. In addition, for both resonances, it was assumed that the magnitude of the transmission coefficient obtained from the simulation $|S_{21}|$ < −40dB. The design process was more complicated due to the multilayers resulting from the technological process used in photolithography. For this reason, it was divided into three stages. In the first stage, initial geometry was estimated based on the literature [21]. In the next step, based on initial geometry, a numerical model was built in the Comsol Multiphysics environment. In the third step, the geometric parameters of the MS were tuned to meet the assumed electromagnetic parameters (f_{r1}, $f_{r2,}$ and $|S_{21}|$). The designed geometry of the square SRR with a description is shown in Figure 1, and the dimensions are listed in Table 1. The obtained characteristics of the reflection coefficient S_{11} and transmission coefficient S_{21} are shown in Figure 2. For both resonances, the electric field distributions are shown, as illustrated in Figures 3 and 4. As can be seen, the highest values of the electric field are in the vicinity of the gap at heights of up to a few micrometers. Adding an additional layer near the gap affects the electric field near the gap and, as a result, the resonant frequencies change. The MS was developed on a silicon (Si) wafer with a low boron content (10–20 Ω cm) and a thickness of 520 μm. This design can be realized using micro process technology, such as layer deposition (SiO_2 and Al) and layer structuring using photolithography and etching processes.

3 Numerical model

The third step of the design and further analyses were conducted using a FEM-based Comsol Multiphysics

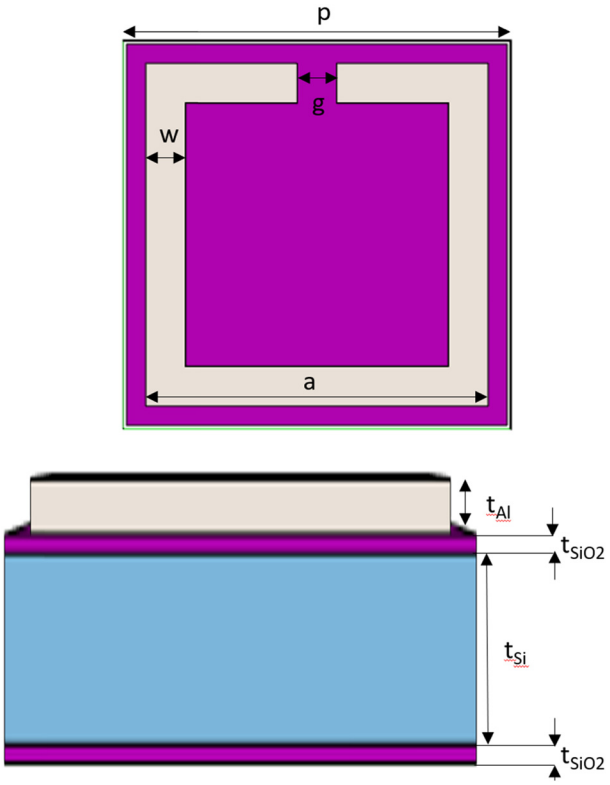

Figure 1: SRR MS dimensions on a silicon wafer with top, and cross-section view; figure not in scale.

Table 1: Dimensions of designed SRR MS

Dimensions	(μm)
Periodicity, p	24.2
Square loop length, a	21.7
Line width, w	2.5
Gap, g	2.5
Aluminum thickness, t_{Al}	0.5
Silicon dioxide thickness, t_{SiO_2}	0.17
Silicon thickness, t_{Si}	520

environment. The model geometry and additional dielectric layer dimensions are illustrated in Figure 5. The following configuration of basic parameters was used: foil (additional dielectric layer) thickness $t_f = 20$ μm, foil permittivity $\epsilon_r = 2$, and foil suspension height $h_s = 0$ μm. The following values of MS dielectric properties were assumed for utilized materials. The permittivity of silicon is $\varepsilon_{rSi} = 12.11$. The real and imaginary parts of silicon dioxide complex permittivity for the terahertz range are $\varepsilon'_{rSiO_2} = 4.45$ and $\varepsilon''_{rSiO_2} = 0.03$, respectively [22]. The value of the aluminum refractive index n_{Al} was described by a Drude model [23].

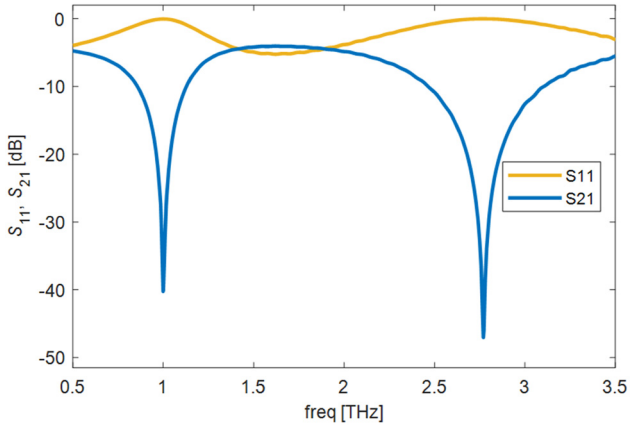

Figure 2: Reflection and transmission coefficient for designed MS.

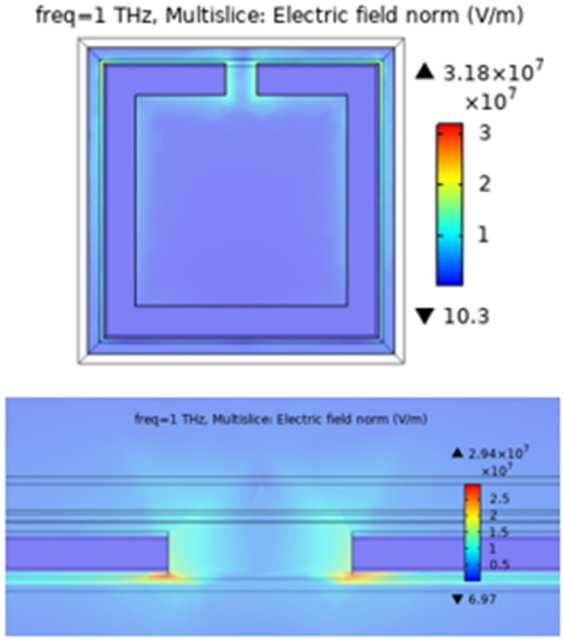

Figure 3: Electric field distribution for the first resonant frequency with top and near the gap view.

$$n_{Al} = \sqrt{\varepsilon'_{rAl} + i\varepsilon''_{rAl}} = \sqrt{1 - \frac{\omega_p^2}{\omega^2 + \gamma^2} + i\frac{\omega_p^2 \gamma}{\omega_p^3 + \gamma^2 \omega}}, \quad (1)$$

where $\omega_p = 2.123 \times 10^{16}$ rad/s is the plasmon frequency of metal; it depends on the density of free electrons in the metal, electron charge, electron mass, and dielectric constant in a vacuum (for aluminum it is 2.123×10^{16} rad/s), ω is the angular frequency of the incidence wave, and $\gamma = 1.975 \times 10^{11}$/s is the damping coefficient of the aluminum.

The electromagnetic wave was excited on Port 1, while received on Port 2 enabling the calculation of the S_{21} transmission coefficient. The reflection coefficient S_{11}

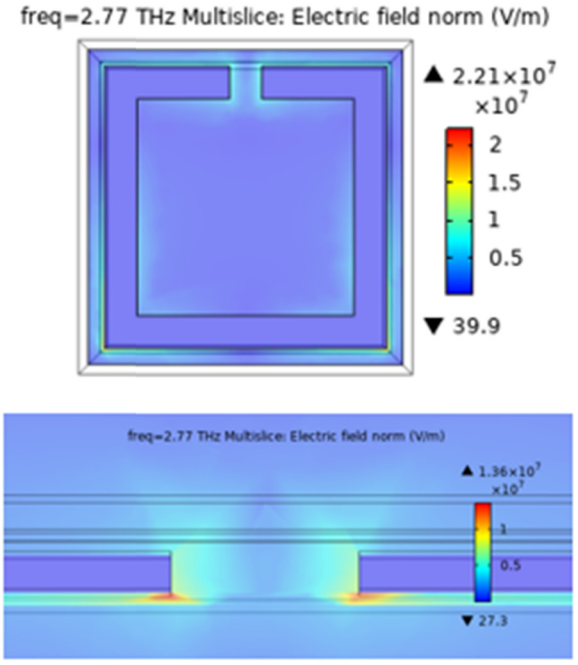

Figure 4: Electric field distribution for the second resonant frequency with top and near the gap view.

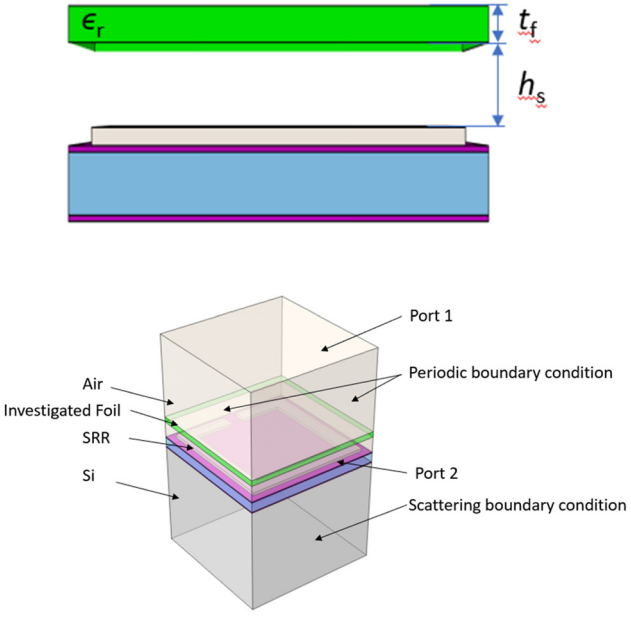

Figure 5: Schematic view of the numerical model.

was calculated on Port 1. The side walls were given the Floquet-periodic boundary conditions to reduce the computational complexity. The application of an additional dielectric layer of various thicknesses, dielectric parameters, and suspension heights does not affect the model symmetry; thus, this allowed us to analyze just a single structural element.

In the considered electromagnetic problem, the following frequency domain equation is solved [24]:

$$\nabla \times \mu_r^{-1}(\nabla \times E) - k_0^2\left(\varepsilon_r - \frac{j\sigma_e}{\omega\varepsilon_0}\right)E = 0, \qquad (2)$$

where μ_r – relative permeability, E – electric field, k_0 – wave number, ε_r – relative permittivity, σ_e – electric conductivity, ω – angular frequency, and ε_0 – permittivity of vacuum.

4 Analysis

During the analysis of the dielectric layer influence, its thickness, permittivity, and suspension height over the MS were evaluated. Changes in the values of two resonant frequencies were analyzed (Figures 6 and 7). For a clearer analysis, the resonant frequency shift parameter was introduced:

$$\Delta f_{r1} = f_{r1\_tf} - f_{r1\_t\text{fair}}, \quad \Delta f_{r2} = f_{r2\_tf} - f_{r2\_t\text{fair}}, \qquad (3)$$

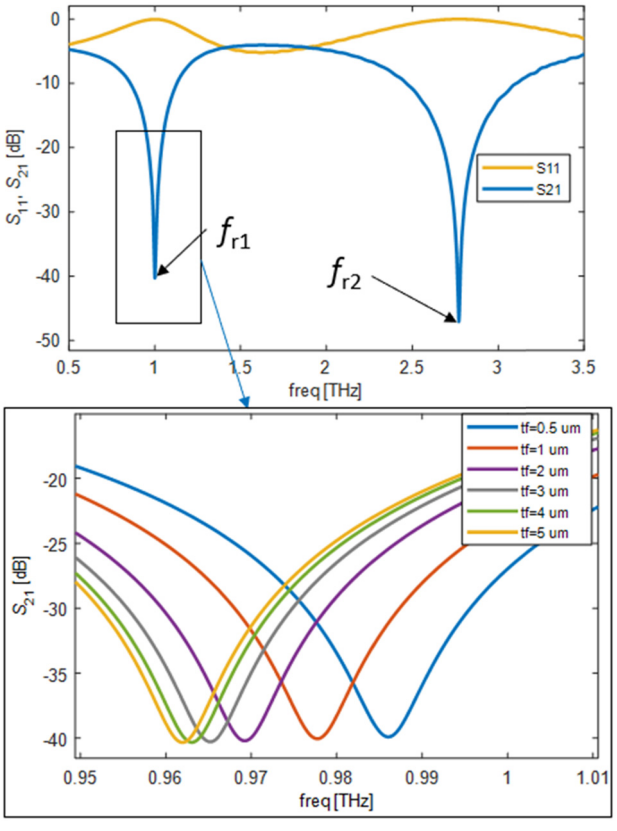

Figure 6: Analyzed frequencies (top); an exemplary set of characteristics for dielectric layer (foil) thickness analysis (bottom); h_s = 0 µm.

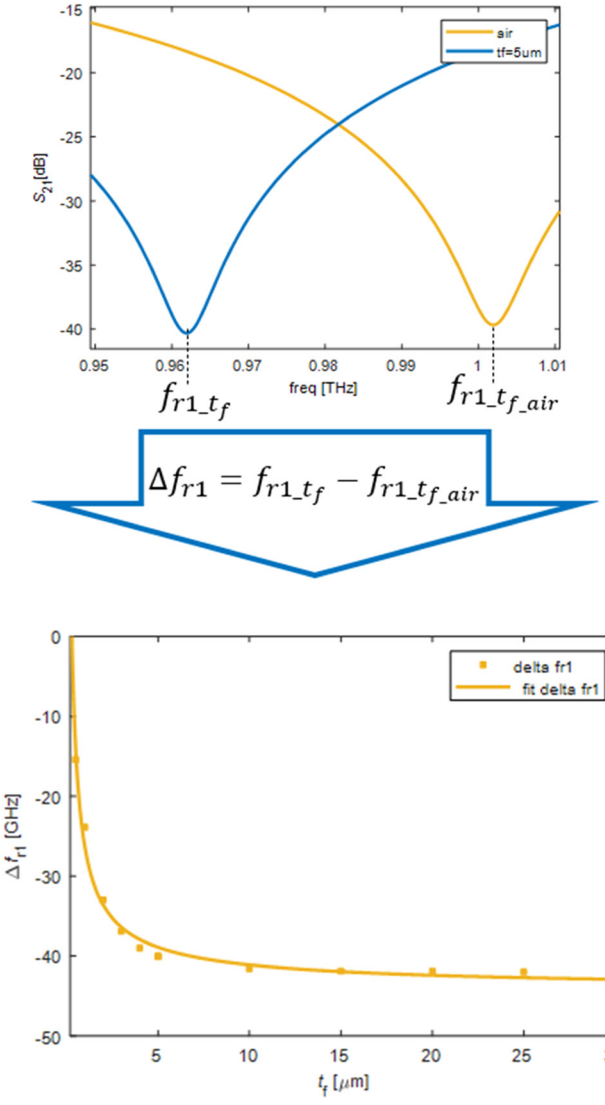

Figure 7: Principle of determining resonant frequency shift.

where Δf_{r1} and Δf_{r2} – resonant frequencies of absolute shifts, f_{r1_tfair} and f_{r2_tfair} – resonant frequencies of MS without the presence of additional thin layer, and f_{r1_tf} and f_{r2_tf} – resonant frequencies of MS with the presence of additional thin layer. The principle of determining this parameter is shown in Figure 7.

An example set of characteristics obtained for the increase in the film thickness in the case of the first resonant frequency is presented in Figure 6 (bottom). The film thickness analysis was carried out in the range from 0.5 to 30 µm, the results of the analysis in the case of both resonances are shown in Figure 8. It is clearly seen that the change in thickness until about 5 µm affects both resonant frequencies, but for thicker layers, this effect saturates, and no further changes are observed (because

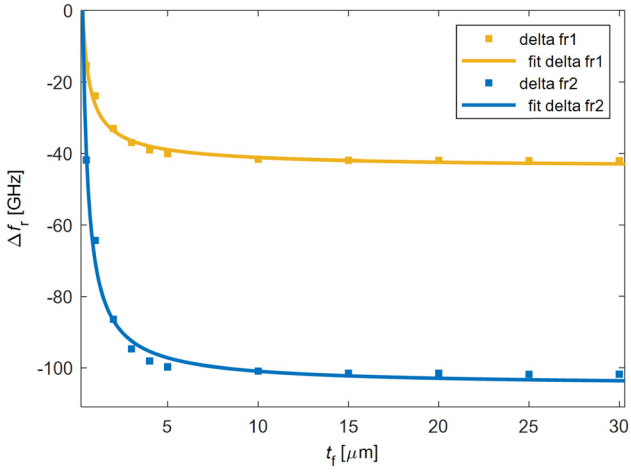

Figure 8: Results of foil thickness analysis.

of electric field distribution – concentration in the vicinity of resonator's gap – in a plane perpendicular to MS plane). In the case of studying the effect of the relative permittivity of the film, its value varied from 1 to 9. The results of this analysis are shown in Figure 9. In the case of both resonances, quasi-linear relationships were obtained. Meanwhile, in the third analysis, the value of the film suspension height was changed from 0 to 50 µm. The results of this analysis are shown in Figure 10. Here as in the case of the layer thickness analysis, visible changes in resonance frequencies occur for distances up to about 5 µm. Similarly, like in the case of layer thickness analysis, this is due to the distribution (range) of the electric field induced in the capacitive gaps of the ring resonators. For bigger heights, both resonant frequencies remain unchanged.

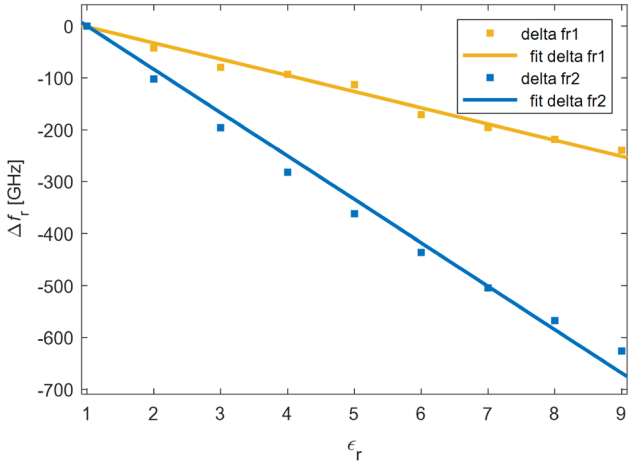

Figure 9: Results of foil relative permittivity analysis.

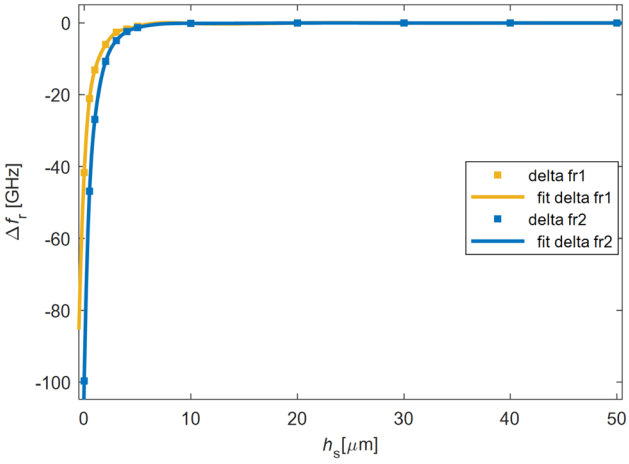

Figure 10: Results of foil suspension height analysis.

5 Conclusion

This work presents research on the influence of an additional thin dielectric layer and its parameters on the transmission properties of the MS for electromagnetic waves in the terahertz range. Resonant frequencies of two basic resonances occurring in the MS based on the rectangular SRR were adopted as the determinant of the observed changes. Relatively high sensitivity to changes in layer thickness below 5 µm was found. For thicker layers, due to the depth of penetration of electromagnetic fields in the vicinity of the structural element, the effect of changing the resonant frequency, and thus the impact on the MS resonance properties, disappears.

For the analyzed structural element, an additional dielectric layer should be suspended at most 6 µm above the MS surface. The greater height of the suspension does not significantly change any of the resonance frequencies.

The increase in electric permeability of the tested layer causes an increase in the deviation of both resonance frequencies, while for f_{r2}, the increase is greater. In both cases, this relationship is linear.

The dependencies regarding the thickness and height of suspension of the additional layer depend on the electric permeability as well as on the electromagnetic parameters of the MS and its operating frequency (the lower the resonance frequency, the longer the corresponding wavelength, and the greater the height of suspension and layer thickness that can be evaluated).

Theoretically, changing the parameters of an additional dielectric layer can be an efficient mechanism for changing the properties of a reconfigurable MS. Tuning the height of the suspension of the layer allows you to change the resonant frequency by 100 GHz, thickness by 40 GHz (f_{r1}) and 100 GHz (f_{r2}), while the change in dielectric permittivity by 250 GHz (f_{r1}) and 650 GHz (f_{r2}). In fact, a change in thickness is practically impossible to apply, a change in the height of the suspension could be achieved by the MEMS structure, while a change in dielectric permittivity can be achieved by using materials with variable dielectric properties (this unfortunately, concerns a narrow range of changes).

If we consider the presented analysis from the point of view of how the protective coating affects the operation of the designed MS, h_s = 0 µm should be considered. Therefore, for the adopted geometry of the structural element, it should be assumed that both resonant frequencies will decrease by nearly 100 GHz compared to MS without protective coating.

Moreover, the evident relation between resonant frequencies and layer thickness, and dielectric parameters, makes this configuration very efficient in the case of nondestructive evaluation of thin foils including thickness monitoring, defects detection, and homogeneity monitoring. However, in the case of this application, great effort should be made to guarantee a constant lift-off value (h_s = const.).

Funding information: This work was done within the project "RE-TERA- Reconfigurable terahertz devices for EM waves manipulation and sensing applications" co-financed by the Polish National Agency for Academic Exchange (NAWA, Poland) and German Academic Exchange Service (DAAD, Germany), under the grant no. PPN/BDE/2021/1/00012/U/ 00001, ID: 57602825.

Conflict of interest: Authors state no conflict of interest.

References

[1] Valipour A, Kargozarfard MH, Rakhsi M, Yaghootian A, Sedighi HM. Metamaterials and their applications: An overview. Proc Inst Mech Eng L. 2021;236(11):1–40. doi: 10.1177/1464420721995858.

[2] Engheta N, Alu A, Silveirinha MG, Salandrino A, Li J. DNG, SNG, ENZ and MNZ metamaterials and their potential applications. Malaga, Spain: 2006, May 16–19. doi: 10.1109/MELCON.2006.1653087.

[3] Lopato P, Herbko M. Evaluation of selected metasurfaces' sensitivity to planar geometry distortions. Appl Sci. 2020;10(1):261. doi: 10.3390/app10010261.

[4] Gric T, Hess O. Metamaterial cloaking. In: Gric T, Hess O, editors. Micro and nano technologies, phenomena of optical metamaterials. Amsterdam: Elsevier; 2019. 175–86. doi: 10.1016/B978-0-12-813896-0.00007-9.

[5] Yang F, Pitchapp P, Wang N. Terahertz reconfigurable intelligent surfaces (RISs) for 6G communication links. Micromachines. 2022;13(2):285. doi: 10.3390/mi13020285.
[6] Xu C, Ren Z, Wei J, Lee C. Reconfigurable terahertz metamaterials: From fundamental principles to advanced 6G applications. iScience. 2022;25(2):103799. doi: 10.1016/j.isci.2022.103799.
[7] Yang J, Qi L, Li B, Wu L, Shi D, Uqaili JA, et al. A terahertz metamaterial sensor used for distinguishing glucose concentration. Results Phys. 2021;26(6):104332. doi: 10.1016/j.rinp.2021.104332.
[8] Bhati R, Malik AK. Ultra-efficient terahertz metamaterial sensor. Results Opt. 2022;8:100236. doi: 10.1016/j.rio.2022.100236.
[9] Li X, Zheng G, Zhang G, Yang J, Hu M, Li J, et al. Highly sensitive terahertz dielectric sensor for liquid crystal. Symmetry. 2022;14(9):1820. doi: 10.3390/sym14091820.
[10] Baxter JB, Guglietta GW. Terahertz spectroscopy. Anal Chem. 2021;83(12):4342–68. doi: 10.1021/ac200907z.
[11] Lopato P. Double-sided terahertz imaging of multilayered glass fiber-reinforced polymer. Appl Sci. 2017;7(7):661. doi: 10.3390/app7070661.
[12] Fukunaga K, Ogawa Y, Hayashi S, Hosako I. Terahertz spectroscopy for art conservation. IEICE Electron Express. 2007;4(8):258–63. doi: 10.1587/elex.4.258.
[13] Spies JA, Neu J, Tayvah UT, Capobianco MD, Pattengale B, Ostresh S, et al. Terahertz spectroscopy of emerging materials. J Phys Chem C. 2020;124(41):22335–46. doi: 10.1021/acs.jpcc.0c06344.
[14] Piegari A, Masetti E. Thin film thickness measurement: A comparison of various techniques. Thin Solid Films. 1985;124(3–4):249–57. doi: 10.1016/0040-6090(85)90273-1.
[15] Bai J, Li J, Wang X, Zhou Q, Ni K, Li X. A new method to measure spectral reflectance and film thickness using a modified chromatic confocal sensor. Opt Lasers Eng. 2022;154(6):107019. doi: 10.1016/j.optlaseng.2022.107019.
[16] Du Y, Yan H, Wu Y, Yao X, Nie Y, Shi B. Non-contact thickness measurement for ultra-thin metal foils with differential white light interferometry. Chin Opt Lett. 2004;2(12):701–3.
[17] Bolivar PH, Brucherseifer M, Rivas JG, Gonzalo R, Ederra I, Reynolds AL, et al. Measurement of the dielectric constant and loss tangent of high dielectric-constant materials at terahertz frequencies. IEEE Trans Microw Theory Techn. 2003;51(4):1062–6. doi: 10.1109/TMTT.2003.809693.
[18] Park SJ, Yoon SAN, Ahn YH. Dielectric constant measurements of thin films and liquids using terahertz metamaterials. RSC Adv. 2016;6(73):69381–6. doi: 10.1039/C6RA11777E.
[19] Park SJ, Ahn YH. Accurate measurement of THz dielectric constant using metamaterials on a quartz substrate. Curr Opt Photon. 2017;1(6):637–41. doi: 10.3807/COPP.2017.1.6.637.
[20] Gora P, Lopato P. Thin dielectric layers evaluation using tunable split-ring resonator based metasurface in THz frequency range. Appl Sci. 2022;12(17):8526. doi: 10.3390/app12178526.
[21] Marqués R, Martin F, Sorolla M. Metamaterials with negative parameters: Theory, design, and microwave applications. Hoboken, New Jersey: John Wiley & Sons; 2008.
[22] Fujii T, Ando A, Sakabe Y. Characterization of dielectric properties of oxide materials in frequency range from GHz to THz. J Eur Ceram Soc. 2006;26:1857–60.
[23] Sun W-F, Wang X-K, Zhang Y. Measurement of refractive index for high reflectance materials with terahertz time domain reflection spectroscopy. Chin Phys Lett. 2009;26(11):114210.
[24] Frei W. Modeling of Materials in Wave Electromagnetics Problems, Comsol Blog; 2015. https://www.comsol.com/blogs/modeling-of-materials-in-wave-electromagnetics-problems/, access 9.09.2022.